JCB Article

The SH2-containing inositol polyphosphate 5-phosphatase, SHIP-2, binds filamin and regulates submembraneous actin

Jennifer M. Dyson,[1] Cindy J. O'Malley,[1] Jelena Becanovic,[1] Adam D. Munday,[1] Michael C. Berndt,[2] Imogen D. Coghill,[1] Harshal H. Nandurkar,[1] Lisa M. Ooms,[1] and Christina A. Mitchell[1]

[1]Department of Biochemistry and Molecular Biology, Monash University, Clayton, Victoria, 3800 Australia
[2]Baker Medical Research Institute, Prahran, Victoria, 3181 Australia

SHIP-2 is a phosphoinositidylinositol 3,4,5 trisphosphate (PtdIns[3,4,5]P_3) 5-phosphatase that contains an NH_2-terminal SH2 domain, a central 5-phosphatase domain, and a COOH-terminal proline-rich domain. SHIP-2 negatively regulates insulin signaling. In unstimulated cells, SHIP-2 localized in a perinuclear cytosolic distribution and at the leading edge of the cell. Endogenous and recombinant SHIP-2 localized to membrane ruffles, which were mediated by the COOH-terminal proline–rich domain. To identify proteins that bind to the SHIP-2 proline–rich domain, yeast two-hybrid screening was performed, which isolated actin-binding protein filamin C. In addition, both filamin A and B specifically interacted with SHIP-2 in this assay. SHIP-2 coimmunoprecipitated with filamin from COS-7 cells, and association between these species did not change after epidermal growth factor stimulation. SHIP-2 colocalized with filamin at Z-lines and the sarcolemma in striated muscle sections and at membrane ruffles in COS-7 cells, although the membrane ruffling response was reduced in cells overexpressing SHIP-2. SHIP-2 membrane ruffle localization was dependent on filamin binding, as SHIP-2 was expressed exclusively in the cytosol of filamin-deficient cells. Recombinant SHIP-2 regulated PtdIns(3,4,5)P_3 levels and submembraneous actin at membrane ruffles after growth factor stimulation, dependent on SHIP-2 catalytic activity. Collectively these studies demonstrate that filamin-dependent SHIP-2 localization critically regulates phosphatidylinositol 3 kinase signaling to the actin cytoskeleton.

Introduction

Phosphoinositides are ubiquitous membrane components which regulate proliferation, differentiation, inhibition of apoptosis, secretion, cell movement, and the actin cytoskeleton. Receptor-regulated phosphoinositide 3 (PI-3)* kinases phosphorylate phosphatidylinositol 4,5 bisphosphate (PtdIns[4,5]P_2) forming phosphatidylinositol 3,4,5 trisphosphate (PtdIns[3,4,5]P_3) that is dephosphorylated by the inositol polyphosphate 5-phosphatases (5-phosphatase) to PtdIns(3,4)P_2 (Majerus, 1996; Martin, 1997). Both PtdIns (3,4,5)P_3 and PtdIns(3,4)P_2 localize signaling proteins to the inner wall of the plasma membrane and allosterically regulate these target proteins. PtdIns(3,4,5)P_3 and PtdIns(3,4)P_2 binding proteins include the serine/threonine kinase, Akt, which inhibits apoptosis, and proteins such as cytohesins and centaurins that regulate ADP ribosylation factor (ARF), and thereby vesicular trafficking and the peripheral actin cytoskeleton (Corvera et al., 1999; Datta et al., 1999). PtdIns(3,4,5)P_3 regulates growth factor–induced actin-dependent extension of lamellipodia, membrane ruffle formation, and cell migration.

PtdIns(3,4,5)P_3 is metabolized by the removal of either the 5- or 3-position phosphate by specific 5- or 3-lipid phosphatases, respectively. The product of the tumor suppressor gene phosphatase and tensin homologue deleted on chromosome 10 (PTEN) is a PtdIns(3,4,5)P_3 3-phosphatase which hydrolyses PtdIns(3,4,5)P_3, forming PtdIns(4,5)P_2. The lipid 3-phosphatase activity of PTEN is critical for its tumor suppressor function (for review see Cantley and Neel, 1999).

The 5-phosphatases hydrolyze the 5-position phosphate from both inositol phosphates and phosphoinositides and share the

Address correspondence to Christina A. Mitchell, Dept. of Biochemistry and Molecular Biology, Monash University, Clayton, Victoria, 3800 Australia. Tel.: (61) 3990-53790. Fax: (61) 3990-54699. E-mail: christina.mitchell@med.monash.edu.au

*Abbreviations used in this paper: aa, amino acid; 5-phosphatase, inositol polyphosphate 5-phosphatase; FLNC, filamin C; GFP, green fluorescent protein; HA, hemagglutinin; PH, pleckstrin homology; PI-3, phosphatidylinositol 3; PtdIns, phosphatidylinositol; PTEN, phosphatase and tensin homologue deleted on chromosome 10; SHIP, SH2 domain–containing inositol polyphosphate 5-phosphatase.

Key words: SHIP-2; inositol polyphosphate 5-phosphatase; filamin; cytoskeleton; phosphatidylinositol 3,4,5-trisphosphate

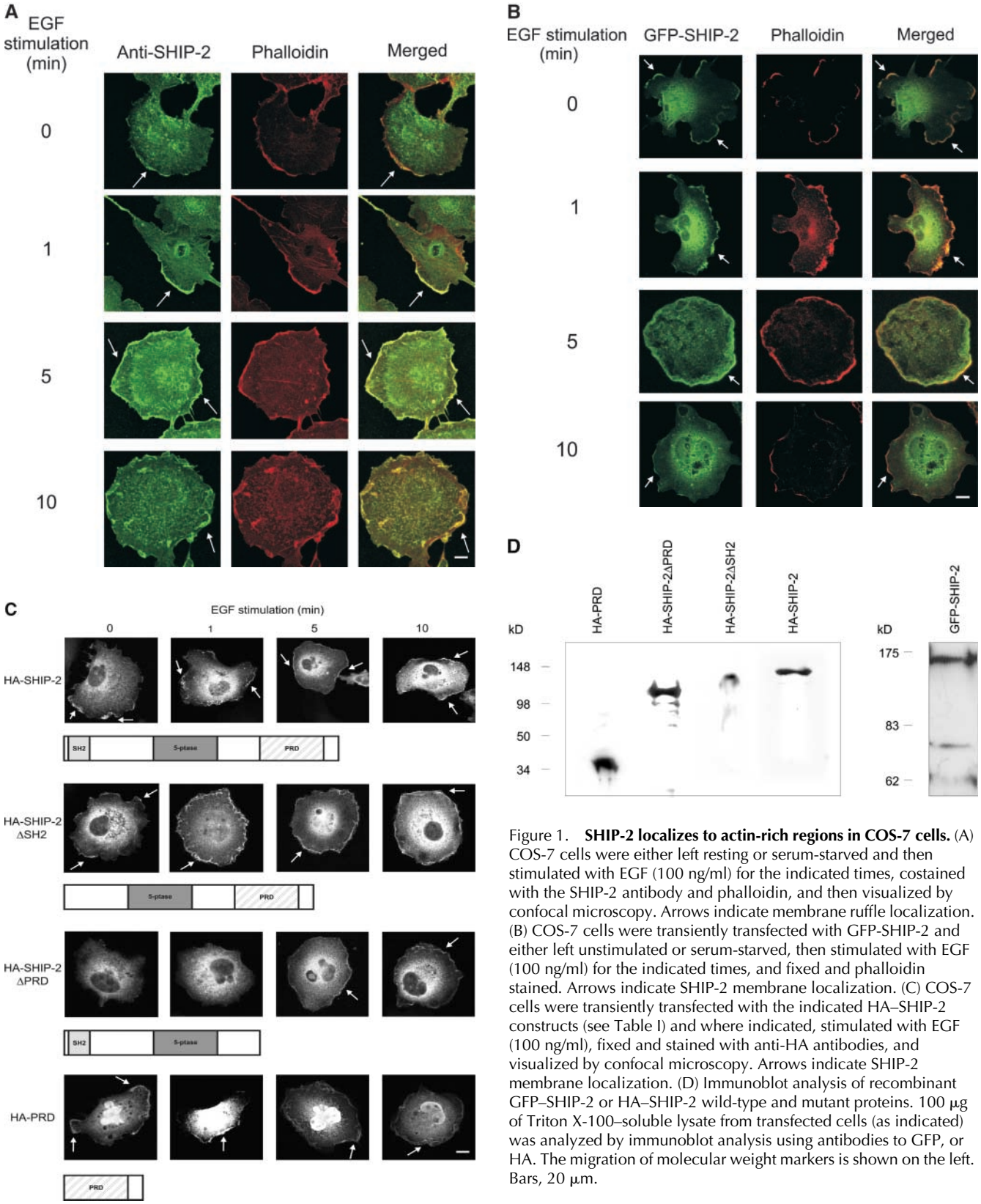

Figure 1. **SHIP-2 localizes to actin-rich regions in COS-7 cells.** (A) COS-7 cells were either left resting or serum-starved and then stimulated with EGF (100 ng/ml) for the indicated times, costained with the SHIP-2 antibody and phalloidin, and then visualized by confocal microscopy. Arrows indicate membrane ruffle localization. (B) COS-7 cells were transiently transfected with GFP-SHIP-2 and either left unstimulated or serum-starved, then stimulated with EGF (100 ng/ml) for the indicated times, and fixed and phalloidin stained. Arrows indicate SHIP-2 membrane localization. (C) COS-7 cells were transiently transfected with the indicated HA–SHIP-2 constructs (see Table I) and where indicated, stimulated with EGF (100 ng/ml), fixed and stained with anti-HA antibodies, and visualized by confocal microscopy. Arrows indicate SHIP-2 membrane localization. (D) Immunoblot analysis of recombinant GFP–SHIP-2 or HA–SHIP-2 wild-type and mutant proteins. 100 μg of Triton X-100–soluble lysate from transfected cells (as indicated) was analyzed by immunoblot analysis using antibodies to GFP, or HA. The migration of molecular weight markers is shown on the left. Bars, 20 μm.

same catalytic mechanism to the apurinic/apyrimidinic endonucleases (Majerus, 1996; Whisstock et al., 2000; Tsujishita et al., 2001). SHIP-2 is a widely expressed 5-phosphatase which plays a significant role in negatively regulating insulin signaling (Ishihara et al., 1999; Clement et al., 2001). SHIP-2 contains an NH_2-terminal SH2 domain, a central 5-phosphatase domain, and a COOH-terminal proline–rich domain and bears significant sequence identity with the 5-phosphatase, SHIP-1, except in the proline-rich domain. SHIP-2 hydrolyses the 5-position phosphate from PtdIns(3,4,5)P_3 and PtdIns(4,5)P_2, and in some, but not all, studies has been shown to hydrolyze the soluble inositol

phosphate Ins(1,3,4,5)P_4 (Pesesse et al., 1997; Wisniewski et al., 1999; Taylor et al., 2000). In contrast to SHIP-1, which has a restricted hematopoietic expression, SHIP-2 is widely expressed. SHIP-2 undergoes cytokine-, growth factor–, and insulin-stimulated phosphorylation in a number of cell lines (Habib et al., 1998; Wisniewski et al., 1999). In addition, SHIP-2 is constitutively tyrosine phosphorylated and associated with Shc in chronic myeloid leukemic progenitor cells, suggesting a role for SHIP-2 in $210^{bcr/abl}$-mediated myeloid expansion (Wisniewski et al., 1999). SHIP-2, like PTEN, regulates both PtdIns(3,4,5)P_3-mediated Akt activation and the induction of cell cycle arrest associated with increased stability of expression of the cell cycle inhibitor $p27^{KIPI}$ (Taylor et al., 2000). Recent studies have demonstrated SHIP-2 negatively regulates insulin signaling. Homozygous mice lacking SHIP-2 develop severe neonatal hypoglycemia and prenatal death. Adult SHIP-2 heterozygous mutant mice demonstrate insulin sensitivity associated with increased translocation of GLUT4 to the plasma membrane in response to insulin treatment (Clement et al., 2001).

In this study we examine the intracellular location of the 5-phosphatase SHIP-2 and demonstrate the enzyme is located at membrane ruffles mediated via its proline-rich domain. SHIP-2 forms a complex with the actin binding protein, filamin, and thereby regulates PtdIns(3,4,5)P_3 and actin at the leading edge of the cell. This may represent a mechanism for the tight spatial regulation of PtdIns(3,4,5)P_3 at specific sites after growth factor or insulin stimulation.

Results

Intracellular localization of SHIP-2 in unstimulated and EGF-stimulated cells

We localized endogenous SHIP-2 in both COS-7 cells and NIH3T3 cells (unpublished data) by indirect immunofluorescence using affinity-purified antiserum raised to its unique COOH-terminal sequence. Similar results were found in both cell types. In unstimulated COS-7 cells, SHIP-2 was detected diffusely in the cytosol and concentrated at the plasma membrane at the leading edge of the cell (Fig. 1 A). SHIP-2 colocalized with markers of submembraneous actin, including β-actin (unpublished data) and phalloidin staining. After EGF stimulation, conditions under which membrane ruffles and actin are actively formed and remodeled, SHIP-2 localized initially at membrane ruffles i.e., areas at the edges of lamellipodia where the plasma membrane detaches from the support and rolls up. After 5–10 min EGF stimulation, SHIP-2 was diffusely expressed at the membrane and was detected in areas of active cytoskeletal rearrangement. However, SHIP-2 did not at any time associate with stress fibers, although the enzyme was detected at focal adhesions (unpublished data) as recently reported (Prasad et al., 2001). Preimmune sera were nonreactive (unpublished data). Localization of recombinant SHIP-2 tagged with either green fluorescent protein (GFP) (Fig. 1 B) or hemagglutinin (HA) (Fig. 1 C), matched that of the endogenous protein. In nonstimulated cells, GFP–SHIP-2 was expressed diffusely in the cytosol and in many cells concentrated in a perinuclear distribution. It was also present at the plasma membrane at the leading edge of the cell, colocalizing at this site with phalloidin staining. After EGF stimulation at 1 min, GFP–SHIP-2 concentrated at membrane ruffles, and by 5 min localized diffusely at the plasma membrane, colocalizing as shown in the merged images with phalloidin-staining of actin (Fig. 1 B). We noted membrane ruffling was significantly reduced in many cells overexpressing SHIP-2 (see Fig. 9). Expression of HA-tagged SHIP-2 demonstrated a similar intracellular location to GFP–SHIP-2 (Fig. 1 C). GFP or HA alone were detected diffusely through the cytosol and nucleus and localization did not change after EGF stimulation (unpublished data). Recombinant GFP–SHIP-2 was expressed as a 166-kD protein on SDS-PAGE, with little proteolysis detected (Fig. 1 D).

Identification of peptide sequences mediating SHIP-2 localization to membrane ruffles

SHIP-2 contains an NH_2-terminal SH2 domain, a central catalytic 300 amino acid 5-phosphatase domain, and an extensive COOH-terminal proline–rich domain. To investigate the structural domains mediating SHIP-2 intracellular location, specifically to membrane ruffles, a series of wild-type and mutant SHIP-2 recombinants tagged with HA were expressed in COS-7 cells (Fig. 1 C and Table I). SHIP-2 that lacked the SH2 domain (HA–SHIP-2ΔSH2) localized to membrane ruffles similarly to wild-type SHIP-2 (Fig. 1 C). SHIP-2 that lacked the proline-rich domain (HA–SHIP-2ΔPRD) showed no membrane association in the resting cell and failed to demonstrate membrane ruffle localization after 1 min of EGF stimulation. However, after 5 min of stimulation, faint membraneous localization of HA–SHIP-2ΔPRD was detected, although this was much less intense than the wild-type protein, suggesting that sequences independent of the proline-rich domain may contribute to plasma membrane localization after prolonged growth factor stimulation (Fig. 1 C). This result is consistent with recent studies which have demonstrated SHIP-2 forms a complex with the adaptor protein $p130^{cas}$ via the SH2 domain and localizes to membrane ruffles and focal adhesions after cell adhesion (Prasad et al., 2001). Studies in which only the pro-

Table I. **Oligonucleotides used for the generation of SHIP-2 truncation mutants**

Name of construct	5′ oligonucleotide	3′ oligonucleotide	Polypeptide expressed
HA–SHIP-2 ΔSH2	5′tattctagagagggtgagcgagagccg-3′	5′-atatctagatcaatgatgatgatgatgcttgctgagctgcagggt-3′	5-phosphatase and proline-rich domain (aa 118–1,258 with COOH-terminal hexa HisTag)
HA–SHIP-2 ΔPRD	5′-gtctagaagccaggccccctcctgg-3′	5′-tctagatcatggttcttcaaataacctgg-3′	SH2 domain and 5-phosphatase domain (aa 16–936)
HA-PRD	5′-gtctagagagaaaccgccaccaacgggg-3′	5′-tctagatcatggttcttcaaataacctgg-3′	proline-rich domain (aa 936–1,258)

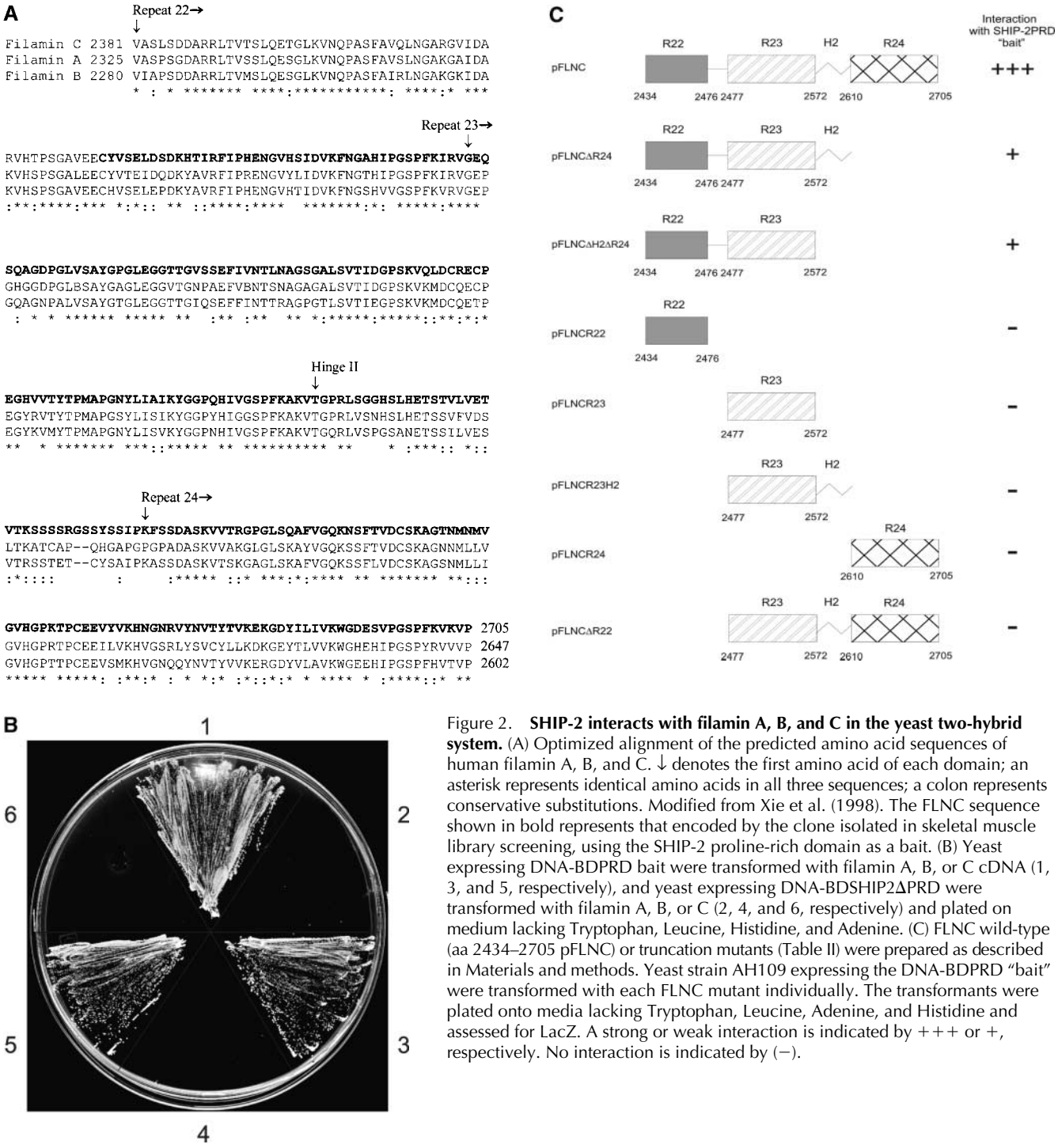

Figure 2. **SHIP-2 interacts with filamin A, B, and C in the yeast two-hybrid system.** (A) Optimized alignment of the predicted amino acid sequences of human filamin A, B, and C. ↓ denotes the first amino acid of each domain; an asterisk represents identical amino acids in all three sequences; a colon represents conservative substitutions. Modified from Xie et al. (1998). The FLNC sequence shown in bold represents that encoded by the clone isolated in skeletal muscle library screening, using the SHIP-2 proline-rich domain as a bait. (B) Yeast expressing DNA-BDPRD bait were transformed with filamin A, B, or C cDNA (1, 3, and 5, respectively), and yeast expressing DNA-BDSHIP2ΔPRD were transformed with filamin A, B, or C (2, 4, and 6, respectively) and plated on medium lacking Tryptophan, Leucine, Histidine, and Adenine. (C) FLNC wild-type (aa 2434–2705 pFLNC) or truncation mutants (Table II) were prepared as described in Materials and methods. Yeast strain AH109 expressing the DNA-BDPRD "bait" were transformed with each FLNC mutant individually. The transformants were plated onto media lacking Tryptophan, Leucine, Adenine, and Histidine and assessed for LacZ. A strong or weak interaction is indicated by +++ or +, respectively. No interaction is indicated by (−).

line-rich domain was expressed (HA-PRD) demonstrated this domain localized to the leading edge of the cell in resting cells, as shown for the wild-type enzyme, and concentrated at membrane ruffles and submembraneous actin–rich structures immediately after EGF stimulation. After 5-min stimulation, however, expression at the membrane was less intense than the wild-type enzyme (Fig. 1 C). Wild-type and mutant HA–SHIP-2 proteins were expressed intact with little proteolysis and migrated at their predicted molecular mass (Fig. 1 D). Collectively, these studies demonstrate that the proline-rich domain mediates SHIP-2 membrane ruffle localization in the resting and in EGF-stimulated cells. In addition, sequences such as the SH2 domain may contribute to membrane localization after prolonged growth factor stimulation.

Identification of SHIP-2 binding partners using yeast two-hybrid analysis

The SHIP-2 COOH-terminal proline–rich domain contains numerous "PXXP" motifs which conform to consensus sequences for SH3 binding domains, 1 WW binding domain motif (PPLP) which may bind to WW domain-containing proteins, and one EVH1 binding domain motif (E/DFPPPPXD/E) which may link the cytoskeletal network to signal transduction pathways (Fedorov et al., 1999). The SHIP-2

proline–rich domain sequence demonstrates no significant sequence homology over the extreme COOH-terminal 322 amino acids with SHIP-1. We searched for proteins that specifically interact with the proline-rich domain using yeast two-hybrid analysis. The entire SHIP-2 proline-rich domain (amino acids [aa] 936–1258) was expressed in yeast cells with a library of proteins expressed as fusions with the GAL4 transcription activation domain. Several rounds of screening a human skeletal muscle library (4×10^6 clones) identified a number of interacting clones in which growth on selective media suggested the presence of bona fide interactors for the proline-rich domain. Sequence analysis demonstrated that one clone, an 818 bp fragment, encoded aa 2434–2705 of the last COOH-terminal two and a half immunoglobulin repeats of the cytoskeletal actin-binding protein filamin C (FLNC), which were in frame with the GAL4 activation domain (Fig. 2 A). Filamin is located in the cortical cytoplasm subjacent to the plasma membrane, and binds actin, promoting orthogonal branching of actin filaments and thereby cell migration and membrane stability (reviewed by Stossel et al., 2001). Filamin forms a complex with a variety of cell surface receptors including FcγRI, the platelet von Willebrand factor receptor, glycoprotein Ib-IX-V, β_1 and β_2 integrin receptors, and intracellular proteins involved in various signaling cascades including Traf 2, granzyme B, caveolin-1, and the stress-activated protein kinase (reviewed by Stossel et al., 2001).

Three human gene filamin paralogues have been identified. Filamin A encodes α-filamin (also called ABP-280) (Gorlin et al., 1990), filamin B codes for β-filamin (also called ABP-278) (Takafuta et al., 1998; Xu et al., 1998), and FLNC encodes for γ-filamin (also called ABPL or FLN2), which is highly expressed in skeletal muscle (Xie et al., 1998). In addition, differential splicing has been demonstrated for each gene (Maestrini et al., 1993; Xie et al., 1998; Xu et al., 1998). All three filamin isoforms demonstrate a similar structure comprising an NH_2-terminal actin binding domain followed by 24 immunoglobulin-like repeat domains creating an extended rod like structure. The extreme COOH-terminal repeat 24 contains a homodimerization domain which is linked to other repeats by a calpain-sensitive "hinge II region" (reviewed by Stossel et al., 2001). As each of the three filamin isoforms shows significant sequence identity in the COOH-terminal region (Fig. 2 A), we investigated if each isoform interacted in cotransformation assays with the proline-rich domain expressed in frame with the DNA binding domain of GAL4 (DNA-BDPRD), or with recombinant mutant SHIP-2 which lacked the proline-rich domain (DNA-BDSHIP-2ΔPRD), versus control heterologous baits. The proline-rich domain "bait" (DNA-BDPRD), but not the SHIP-2 "bait" lacking the proline-rich domain (DNA-BD-SHIP-2ΔPRD), interacted with the COOH-terminal four immunoglobulin repeats of filamin A and B, and the COOH-terminal two and a half immunoglobulin repeats of FLNC, indicated by expression of all three reporter genes *HIS3* and *ADE2* (Fig. 2 B) and *LacZ* (unpublished data).

Identification of FLNC sequences mediating interaction with SHIP-2

To determine the region of FLNC specifically interacting with SHIP-2, a series of wild-type and mutant FLNC constructs comprising the COOH-terminal immunoglobulin repeat regions R22–R24 (aa 2434–2705), which include a "hinge II region" between R23 and R24, were cloned into the activation domain and cotransformed with the DNA-BD-PRD bait and interactions scored as strong (+++), or weak (+) (Fig. 2 C). The fragment containing FLNC repeats 22–24 demonstrated the strongest binding to the proline-rich domain bait. FLNC repeats 23 and 24, either alone or in combination, did not interact with SHIP-2. Repeats 22 and 23 in combination, with or without the hinge II region, interacted with SHIP-2; however, this was weaker than repeats 22–24 (Fig. 2 C). All FLNC truncation mutants were expressed in the yeast strain AH109 and were soluble (unpublished data).

We took several approaches to verify whether SHIP-2 interacted with filamin in vivo and thereby regulated the

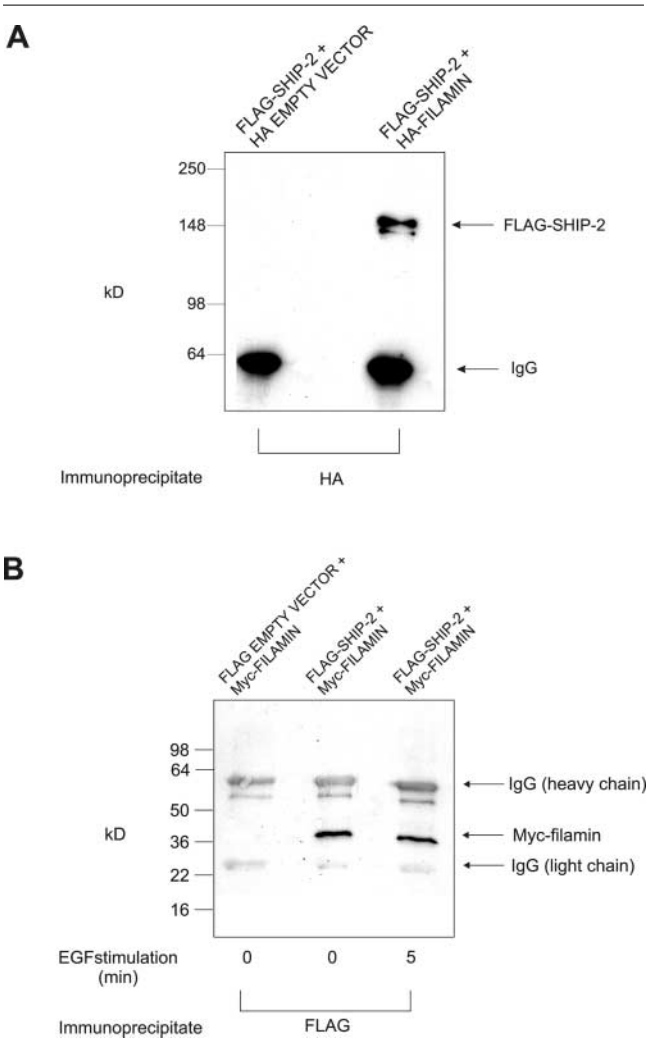

Figure 3. **SHIP-2 associates with filamin in resting and EGF-stimulated COS-7 cells.** (A) COS-7 cells were transiently cotransfected with FLAG–SHIP-2 and HA empty vector, or FLAG–SHIP-2 and HA-filamin (encoding aa 2,434 to 2,705). Cells were harvested and the Triton X-100–soluble lysate was immunoprecipitated with HA antibodies and immunoblotted with FLAG antibodies. (B) COS-7 cells were transiently cotransfected with FLAG empty vector and Myc-filamin (encoding aa 2,434–2,705), or FLAG–SHIP-2 and Myc-filamin. Where indicated, COS-7 cells were EGF treated (100 ng/ml) for 5 min. Cells were harvested and the Triton X-100–soluble lysate was immunoprecipitated with FLAG antibodies and immunoblotted with Myc antibodies.

membrane localization of SHIP-2. First, we investigated using cotransfection and coimmunopreciptation assays if filamin interacted with SHIP-2 in COS-7 cells. We also determined association of endogenous proteins using immunoprecipitation and immunoblot analysis. Second, we demonstrated colocalization of SHIP-2 and filamin at membrane ruffles in resting and EGF-stimulated COS-7 cells. Third, we showed colocalization of filamin and SHIP-2 in mouse heart and skeletal muscle sections using immunolocalization of both species. Finally, we showed the membrane localization of SHIP-2 is dependent on filamin by determining the intracellular localization of SHIP-2 in cells which do not express filamin.

Association of SHIP-2 and filamin was demonstrated in COS-7 cells, which were cotransfected with FLAG-tagged SHIP-2 and HA-tagged filamin (encoding aa 2434–2705 of FLNC), followed by immunoprecipitation and immunoblot analysis using antibodies to each tag. FLAG–SHIP-2 was detected in HA immunoprecipitates of HA-filamin–transfected cells, but not cells transfected with HA empty vector (Fig. 3 A). We determined the effect of EGF stimulation on association between recombinant SHIP-2 and filamin. COS-7 cells were cotransfected with myc-filamin and FLAG–SHIP-2, and after EGF stimulation for 5 min, Triton X-100–soluble lysates were immunoprecipitated using FLAG antibody and immunoblotted with myc antibody. The level of filamin in SHIP-2 immunoprecipitates was unchanged after 5 min EGF stimulation, compared with nonstimulated cells (Fig. 3 B). These studies were repeated expressing SHIP-2 and filamin as fusion proteins with different tags with similar results (unpublished data).

To confirm a complex between endogenous SHIP-2 and filamin, we transfected recombinant myc-tagged filamin (encoding aa 2434–2705 of FLNC) into COS-7 cells and after EGF stimulation performed immunoprecipitations using SHIP-2 antibodies, or preimmune sera, and immunoblotted with either SHIP-2 antibodies (top), or myc tag antibodies to detect filamin (bottom) (Fig. 4 A). This study demonstrated recombinant filamin formed a stable complex with endogenous SHIP-2 and association did not change after growth factor stimulation. In addition, COS-7 cell Triton X-100–soluble lysates immunoprecipitated using SHIP-2 antibodies and immunoblotted using filamin antibodies demonstrated a 280-kD polypeptide consistent with filamin in SHIP-2 immune, but not preimmune immunoprecipitates (Fig. 4 B). In control studies, immunoblot analysis of COS-7 Triton X-100–soluble cell lysates demonstrated the SHIP-2 and filamin antibodies recognized 148- and 280-kD proteins, respectively, consistent with their predicted molecular weight (Fig. 4 C). Collectively, these studies demonstrate SHIP-2 and filamin form a complex in both resting and EGF-stimulated COS-7 cells and the SHIP-2–filamin complex remains unchanged after growth factor stimulation.

We colocalized endogenous filamin and recombinant SHIP-2 after EGF stimulation of COS-7 cells. In nonstimulated cells filamin was located in the cytosol and at the leading edge of the cell (Fig. 5 A). Although HA–SHIP-2 was expressed in the cytosol and membrane, colocalization with filamin was detected only at the membrane at the leading edge of the cell. After EGF stimulation, filamin localized to

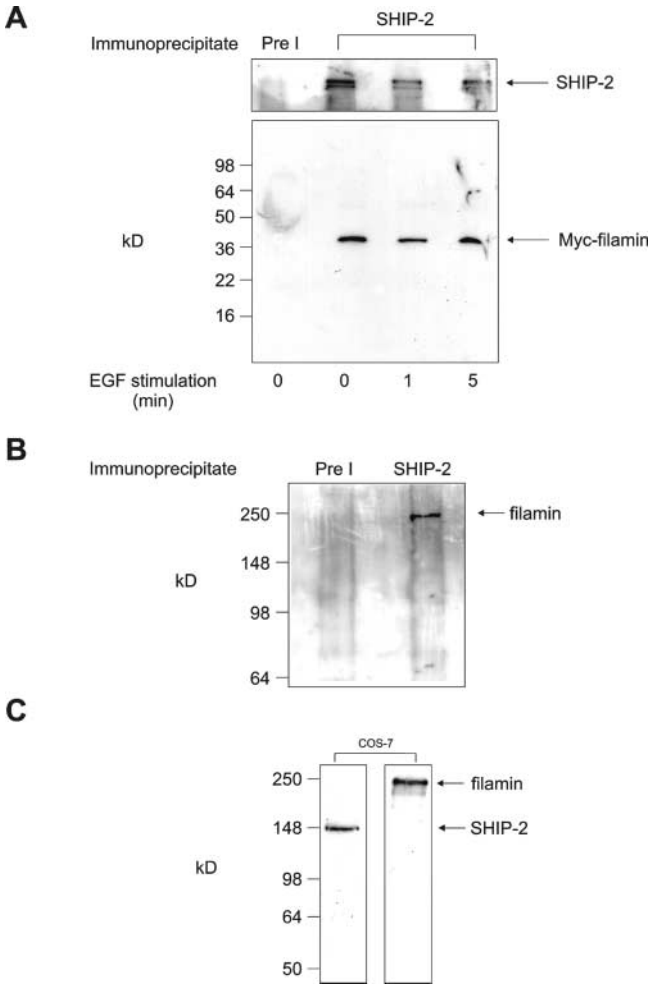

Figure 4. **Endogenous SHIP-2 associates with filamin in COS-7 cells.** (A) COS-7 cells were transiently transfected with Myc-filamin and treated with EGF (100 ng/ml) as indicated. Cells were harvested and the Triton X-100–soluble lysate was immunoprecipitated with either preimmune sera (Pre I) or anti–SHIP-2 sera and immunoblotted with myc antibodies (bottom), then reprobed with anti–SHIP-2 sera to confirm SHIP-2 immunoprecipitation (top). (B) COS-7 cells were harvested and the Triton X-100–soluble lysate was immunoprecipitated with either preimmune sera (Pre I) or anti–SHIP-2 sera and immunoblotted with antibodies to endogenous filamin. (C) COS-7 cells were harvested and 100 μg of the Triton X-100–soluble lysate was immunoblotted with SHIP-2 or filamin antibodies.

a subplasma membrane distribution, initially at membrane ruffles and at the latter time points evenly throughout a fine cortical rim at the periphery of the cell. Filamin colocalized intensely with HA–SHIP-2 at membrane ruffles and the cortical actin rim, but not in the cytosol.

We investigated whether the recombinant COOH-terminal filamin domain (aa 2434–2705) localized as endogenous filamin in COS-7 cells. We also determined whether this recombinant filamin COOH-terminal domain, which represents the SHIP-2 binding site, when expressed at high levels, could displace endogenous SHIP-2 localized at membrane ruffles. The myc-filamin recombinant protein may actually inhibit the localization of SHIP-2 to membrane ruffles by blocking binding to endogenous filamin. In both low and high myc-filamin–expressing cells, the localization of the recombinant protein

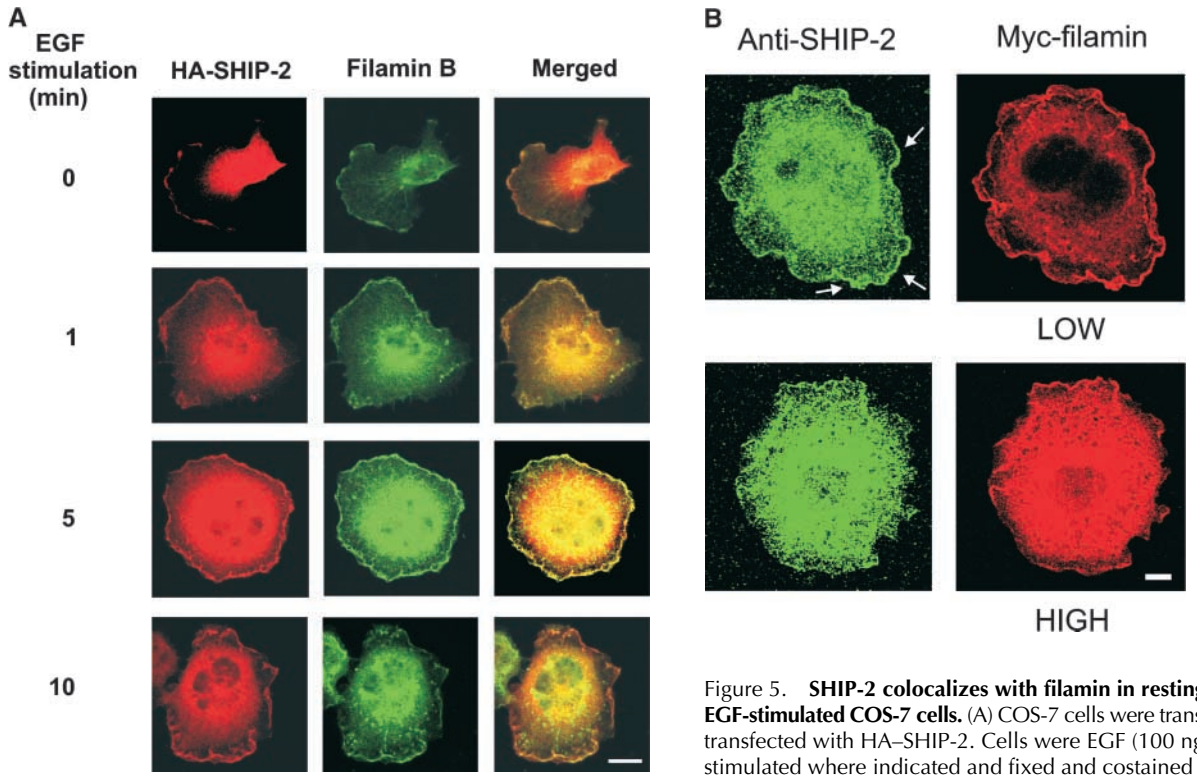

Figure 5. **SHIP-2 colocalizes with filamin in resting and EGF-stimulated COS-7 cells.** (A) COS-7 cells were transiently transfected with HA–SHIP-2. Cells were EGF (100 ng/ml) stimulated where indicated and fixed and costained with HA and filamin B antibodies. Cells were visualized by confocal microscopy. (B) COS-7 cells were transiently transfected with myc-filamin (encoding aa 2,434–2,705) and EGF stimulated for 5 min. Cells were scored as expressing high or low levels of this recombinant protein, as determined by intensity of staining using antibodies to the myc tag by indirect immunofluorescence. The localization of endogenous SHIP-2 was determined using specific SHIP-2 antibodies in cells expressing either low or high levels of myc-filamin. Arrows indicate the localization of SHIP-2 to membrane ruffles. Bars, 20 μM.

matched that of endogenous filamin at membrane ruffles in unstimulated (unpublished data) and more prominently in EGF-stimulated cells (Fig. 5 B). However, in cells expressing myc-filamin at very high levels we noted increased expression of filamin in the cytosol in addition to membrane staining. Localization of endogenous SHIP-2 in myc-filamin–expressing cells was determined by indirect immunofluorescence. In cells expressing low levels of myc-filamin, endogenous SHIP-2 localized to membrane ruffles in both resting (unpublished data) and more prominently in EGF-stimulated cells (Fig. 5 B). In contrast, in cells expressing high levels of myc-filamin, SHIP-2 localized in a perinuclear distribution in the cytosol and staining was less intense at the plasma membrane (Fig. 5 B).

Colocalization of filamin and SHIP-2 in heart and skeletal muscle

FLNC is highly expressed in striated muscle, where it is predominantly localized in myofibrillar Z-discs, with a minor fraction of the protein showing subsarcolemma localization (van der Ven et al., 2000). SHIP-2 is also expressed in skeletal muscle, although its intracellular location in this tissue has not been reported. SHIP-2 homozygous null mice demonstrate increased sensitivity to insulin (Clement et al., 2001). One of the major sites of insulin action is skeletal muscle, where insulin stimulates the translocation of the glucose transporter GLUT4 in a PI-3 kinase–dependent manner to the sarcolemma (Khan et al., 2000). We investigated whether SHIP-2 and filamin colocalized in striated muscle. Mouse heart striated muscle sections were isolated, fixed, and probed with specific affinity purified SHIP-2 antibodies (Fig. 6 A). Soleus muscle showed similar localization (unpublished data). In longitudinal sections SHIP-2 antibodies stained intensively in an alternate banding pattern at areas that resembled Z-lines. No staining of any structure was observed using preimmune serum (Fig. 6 B). Counter-staining sections using antibodies to filamin and the Z-line–specific protein α-actinin demonstrated both colocalized with SHIP-2 (Fig. 6, C–H). Cross-sectional analysis of skeletal muscle demonstrated both filamin and SHIP-2 localized to the sarcolemma, the site of insulin-stimulated GLUT4 translocation (Fig. 6, I–L).

Intracellular localization of SHIP-2 in filamin-deficient cells

To investigate if SHIP-2 membrane ruffle localization was dependent on an interaction with filamin, we examined the intracellular localization of SHIP-2 in a cell line (M2) derived from a human malignant melanoma that does not express detectable filamin messenger RNA or protein (Cunningham et al., 1992). M2 cells demonstrate a distinct phenotype characterized by extensive membrane blebbing and defective locomotion, which is reversed by the stable transfection of filamin A cDNA (A7 subline). Equivalent SHIP-2 expression was demonstrated in A7 and M2 cells as shown by immunoblot analysis using SHIP-2 antipeptide

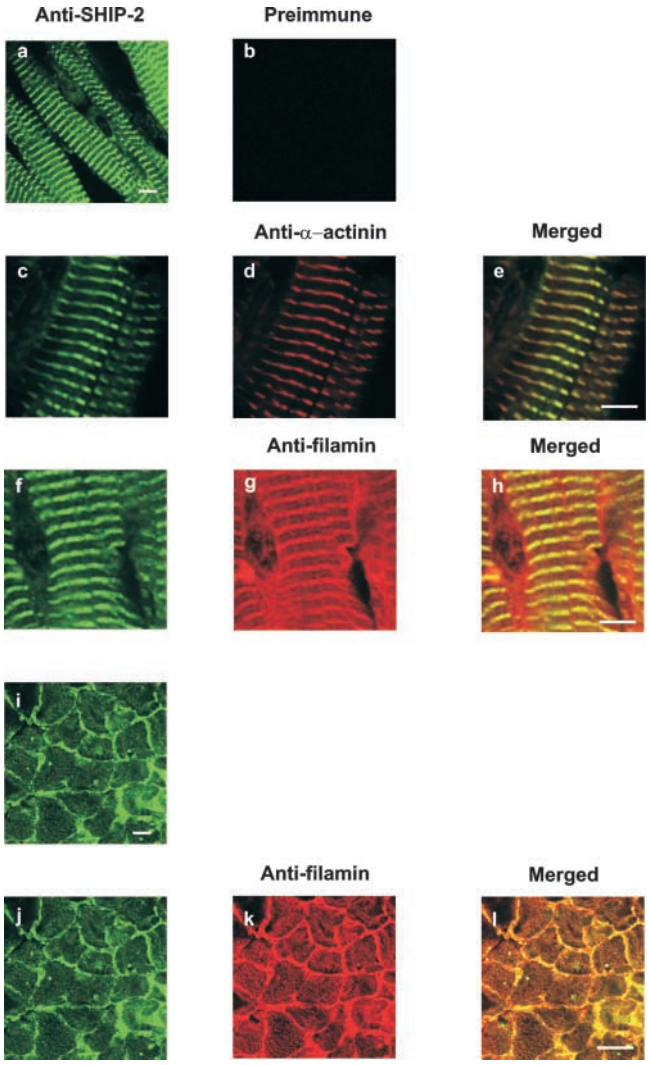

Figure 6. **SHIP-2 colocalizes with filamin at Z-lines in mouse heart and skeletal muscle sections.** Mouse adult heart longitudinal cryosections were cut 7 μm thick and stained with SHIP-2 antibodies (a, c, and f) or preimmune sera (b). SHIP-2 was colocalized with α-actinin (d) at the Z-line and also with antifilamin (g) at the Z-line. Merged images are indicated between SHIP-2 and filamin in panels e and h, respectively. Cross-sectional sections of skeletal muscle were stained with SHIP-2 antibodies (i and j) and counterstained with filamin antibodies (k). Merged images are shown in panel l. Sections were visualized by confocal microscopy. Bars, 20 μm.

antibodies of 100 μg of cell lysate (Fig. 7, A and B). The intracellular localization of SHIP-2 was determined by indirect immunofluorescence of endogenous enzyme using SHIP-2 antipeptide antibodies, or cells transfected with HA-tagged SHIP-2 with detection by staining with antibodies to the tag (unpublished data) with the same result. In nonstimulated M2 cells, SHIP-2 was expressed diffusely in the cytosol and did not colocalize with markers of submembraneous actin such as phalloidin (Fig. 7 A). Upon EGF stimulation, M2 cells transiently form membrane ruffles, or membrane "blebs," which can be detected by phalloidin staining (for review see Stossel et al., 2001). SHIP-2 remained in the cytosol in stimulated cells and did not colocalize with filamin at membrane ruffles. In contrast, in A7 cells, which have been stably transfected with filamin, SHIP-2 localized to membrane ruffles upon EGF stimulation (Fig. 7 B) and colocalized with phalloidin staining. Collectively, these studies demonstrate SHIP-2 localization at membrane ruffles is dependent on filamin expression.

SHIP-2 regulates PtdIns(3,4,5)P_3 and β-actin at membrane ruffles

To establish that recombinant SHIP-2 localized at membrane ruffles was active and to determine the functional consequences on PtdIns(3,4,5)P_3 levels, we employed the pleckstrin homology (PH) domain of ARNO, which has high affinity for PtdIns(3,4,5)P_3 to assess local plasma membrane concentrations of this phosphoinositide (Balla et al., 2000). Several studies have demonstrated that GFP-tagged PH domains with specificity for PtdIns(3,4,5)P_3 can be used to accurately detect PtdIns(3,4,5)P_3 at the leading edge of the cell (for review see Rickert et al., 2000). Although it has been established that SHIP-2 regulates total cellular PtdIns(3,4,5)P_3 levels, the membrane ruffle localized regulation of PtdIns(3,4,5)P_3 has not been reported (Blero et al., 2001; Pesesse et al., 2001). In addition, the functional role of SHIP-2 membrane location in regulating PtdIns(3,4,5)P_3 degradation has not been determined. GFP-fused with the PH domain of ARNO (GFP-PH/ARNO) was coexpressed with either empty vector (HA), or HA–SHIP-2, or the proline-rich domain (HA-PRD), or mutant SHIP-2 which lacked the proline-rich domain (HA–SHIP-2ΔPRD) (Fig. 8). In addition, we determined the effect of overexpressing the COOH-terminal filamin fragment (aa 2434–2705) which binds SHIP-2 in COS-7 cells on PtdIns(3,4,5)P_3 levels, as we have shown overexpression of recombinant myc-filamin displaces endogenous SHIP-2 from membrane ruffles (Fig. 5 B). In nonstimulated cells transfected with HA empty vector and GFP-PH/ARNO, plasma membrane staining of GFP-PH/ARNO was not detected. Upon EGF activation GFP-PH/ARNO translocated rapidly to membrane ruffles after 1 min of stimulation and by 5 min intense plasma membrane staining was detected (Fig. 8). In contrast, cells overexpressing SHIP-2 demonstrated no or low expression of GFP-PH/ARNO at the plasma membrane of EGF-stimulated cells. However, cells expressing the SHIP-2 proline-rich domain (HA-PRD), which lacks the SH2 and catalytic domain, demonstrated strong plasma membrane expression of GFP-PH/ARNO, comparable to HA empty vector expressing cells after EGF stimulation. In cells expressing SHIP-2, which lacks the proline-rich domain (HA-SHIP-2ΔPRD) but contains the SH2 and 5-phosphatase catalytic domain, GFP-PH/ARNO demonstrated growth factor–dependent relocalization to the plasma membrane. However, staining was less intense at 5 min compared with empty vector–expressing cells, but was greater than intact SHIP-2 expressing cells. To confirm these observations, transfected cells were scored as showing high or low GFP-PH/ARNO plasma membrane expression after 5 min of EGF stimulation. Over 40 cells were scored per transfection for three independent experiments by an independent observer. The expression of GFP-PH/ARNO at the plasma membrane was low or not detected in >90% of cells overexpressing SHIP-2, with <10% of cells showing high plasma mem-

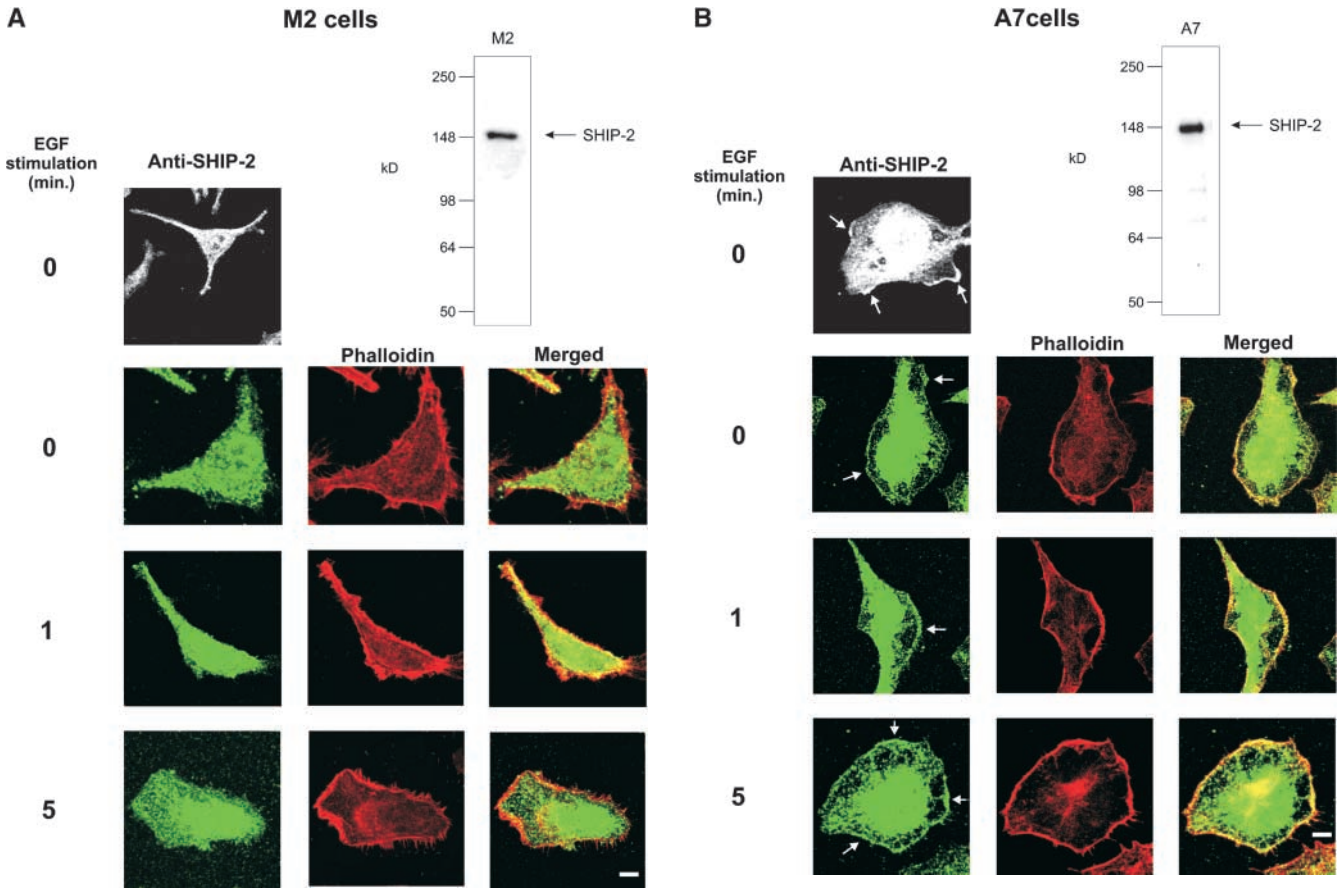

Figure 7. **Filamin is required for membrane localization of SHIP-2.** (A) M2 (filamin-deficient) cells were fixed and costained with phalloidin and anti–SHIP-2 sera. Cells were visualized by confocal microscopy. M2 cells were harvested and 100 μg of the Triton X-100–soluble lysate was immunoblotted with anti–SHIP-2 sera. (B) A7 (filamin-replete) cells were fixed, costained, and immunoblotted as for M2 cells. Arrows indicate SHIP-2 membrane ruffle localization. Cells were visualized by confocal microscopy. A7 cells were harvested and 100 μg of the Triton X-100–soluble lysate was immunoblotted with anti–SHIP-2 sera. Bars, 20 μm.

brane expression of GFP-PH/ARNO. In contrast, 35% of cells in which mutant SHIP-2 lacking the proline-rich domain was overexpressed demonstrated high plasma membrane expression of GFP/ARNO, with 60% of cells demonstrating low expression. In control studies, the majority of cells (>85%) expressing the proline-rich domain demonstrated high expression of GFP/ARNO at the plasma membrane. Finally, the effect of overexpression of myc-filamin on PtdIns(3,4,5)P_3 levels was determined. Cells expressing myc-filamin at high levels demonstrated a dramatic increase in GFP-PH/ARNO staining at the plasma membrane of EGF-treated cells, most apparent after 5 min stimulation. This result is consistent with the contention that expression of this COOH-terminal filamin domain displaces endogenous SHIP-2 from membrane ruffles and therefore leads to enhanced PI-3 kinase signals. Collectively, these studies indicate the SHIP-2–filamin interaction regulates plasma membrane PtdIns(3,4,5)P_3.

PI-3 kinase plays a key role in signaling to the actin cytoskeleton and inducing membrane ruffling via regulation of Rac and Cdc42 (for review see Rickert et al., 2000). As SHIP-2 hydrolyses PtdIns(3,4,5)P_3 and localizes to membrane ruffles via association with filamin, we investigated the regulation of actin at membrane ruffles by this 5-phosphatase. Cells overexpressing SHIP-2 (HA–SHIP-2) or the proline-rich domain of SHIP-2 (HA-PRD), which lacks the catalytic 5-phosphatase domain but localizes to membrane ruffles and complexes with filamin, were stained for submembraneous actin by β-actin immunoreactivity. β-actin is ubiquitously expressed and localizes specifically at the leading edge of the cell at subplasma membrane cortical sites, rather than stress fibers. HA–SHIP-2 colocalized with β-actin in both resting and EGF-stimulated cells (Fig. 9 A). In addition, the intensity of β-actin staining was significantly reduced in cells overexpressing SHIP-2, compared with the SHIP-2 proline-rich domain (Fig. 9 A) or vector alone (unpublished data). To quantitate these differences, cells overexpressing HA–SHIP-2 or the proline-rich domain were scored for the intensity of β-actin staining after EGF stimulation (5 min): 40 cells per transfection for three experiments by an independent observer. Greater than 80% of cells expressing HA–SHIP-2, compared with <20% of cells overexpressing the proline-rich domain which has no 5-phosphatase activity, demonstrated low level β-actin staining. The minority of HA-SHIP-2–expressing cells (<20%) demonstrated intense β-actin staining compared with 75% of cells expressing the proline-rich domain. To further establish whether SHIP-2 regulates submembraneous actin, cells overexpressing HA–SHIP-2 or empty vector were stained with phalloidin which stains polymerized actin (Fig. 9 B). Cells overexpressing high

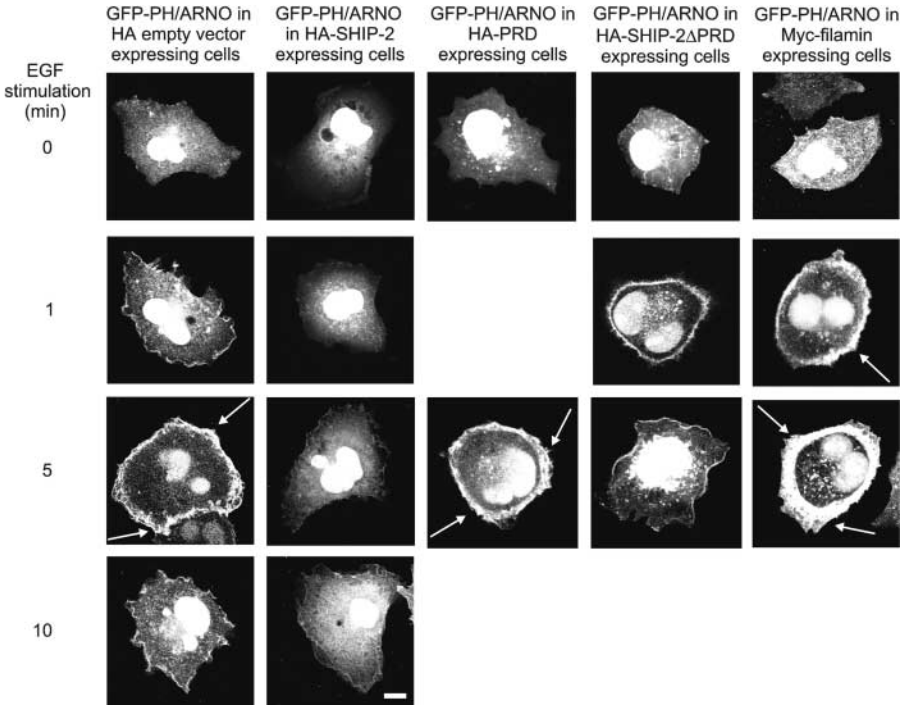

Figure 8. **SHIP-2 regulates PtdIns(3,4,5)P_3 at membrane ruffles.** COS-7 cells were transiently cotransfected with the GFP-PH/ARNO and with either empty vector (HA), HA–SHIP-2, the proline-rich domain (HA-PRD), mutant SHIP-2 which lacked the proline-rich domain (HA–SHIP-2ΔPRD), or Myc-filamin. Cells were EGF treated (100 ng/ml) for the indicated times and stained with HA or Myc antibodies to identify cotransfected cells (unpublished data). Cells were visualized by confocal microscopy for GFP-PH/ARNO expression which is shown. Arrows indicate areas of high GFP-PH/ARNO expression. Bar equals 20 μm.

levels of HA–SHIP-2 demonstrated significantly decreased staining of actin at membrane ruffles and decreased membrane ruffling. In many HA–SHIP-2 overexpressing cells, only a fine cortical rim of actin was stained by phalloidin after 5 min EGF stimulation. The intensity of phalloidin staining of actin at the membrane was scored as high or low after 5 min EGF stimulation in HA–SHIP-2 versus HA empty vector expressing cells for 40 cells per transfection for three independent experiments by an independent observer. Greater than 70% of HA-SHIP-2–expressing cells, compared with 30% of cells expressing the HA empty vector, demonstrated low intensity phalloidin staining at membrane ruffles. In addition, only 25% of SHIP-2 versus 75% of HA empty vector–expressing cells demonstrated high intensity phalloidin staining at membrane ruffles. Collectively, these studies demonstrate SHIP-2 localizes to membrane ruffles via association with filamin and regulates PtdIns(3,4,5)P_3, β-actin, and membrane ruffling.

Discussion

The results of this study demonstrate the 5-phosphatase SHIP-2 forms a functionally significant complex with the actin-binding protein, filamin. SHIP-2 interacts via its proline-rich domain, specifically with filamin A, B, and C isoforms in yeast two hybrid assays. Filamin and SHIP-2 colocalized to Z-lines and the sarcolemma of skeletal muscle, and in mammalian cell lines to membrane ruffles. We demonstrated by reciprocal coimmunoprecipitation studies that SHIP-2 and filamin form a stable complex in COS-7 cells and the level of association between these species does not change after EGF stimulation. SHIP-2 membrane localization is dependent on filamin expression, as membrane association was not detected in a well-characterized melanoma cell line, which does not express filamin. The association of SHIP-2 with filamin serves to regulate PtdIns(3,4,5)P_3 and β-actin at membrane ruffles.

Inositol polyphosphate 5-phosphatases and the cytoskeleton

Increasing evidence indicates that both mammalian and yeast 5-phosphatase isoforms, via hydrolysis of PtdIns(4,5)P_2 and or PtdIns(3,4,5)P_3, play a significant role in regulating cytoskeletal reorganization. The 5-phosphatases comprise 10 mammalian and 4 yeast isoforms with many spliced variants described. Null mutation of any two yeast Sac-1 domain containing 5-phosphatases results in a phenotype which includes disorganization of polymerized actin and delocalization of actin patches from the growing yeast bud to the mother cell (for review see Hughes et al., 2000). The yeast 5-phosphatases, Inp52p and Inp53p, translocate to actin patches upon osmotic stress, the site of plasma membrane invaginations. In addition, overexpression of Inp52p and Inp53p, but not catalytically inactive Inp52p, results in a significant reduction in the repolarization time of actin patches after osmotic stress (Ooms et al., 2000). The mammalian 5-phosphatase, synaptojanin-1, hydrolyses PtdIns(4,5)P_2 bound to the actin regulatory proteins, α-actinin, vinculin, gelsolin, and profilin, and decreases the number of stress fibers in the cell (Sakisaka et al., 1997). Synaptojanin-2 directly interacts with Rac1 in a GTP-dependent manner, resulting in translocation of the 5-phosphatase to membrane ruffles and inhibition of endocytosis (Malecz et al., 2000). Overexpression of SKIP (skeletal muscle and kidney-enriched inositol phosphatase) results in loss of actin stress fibers in areas of SKIP expression (Ijuin et al., 2000). The recently identified proline-rich inositol polyphosphate 5-phosphatase (PIPP) localizes to membrane ruffles, but unlike SHIP-2 does not appear to regulate the actin cytoskeleton (Mochizuki and Takenawa, 1999). SHIP-2 regulation of submembraneous actin levels is most probably mediated via localized regulation of PtdIns(3,4,5)P_3. However, both SHIP-1 and SHIP-2 also hydrolyze PtdIns(4,5)P_2, forming PtdIns(4)P (Kisseleva et al., 2000; Taylor et al., 2000).

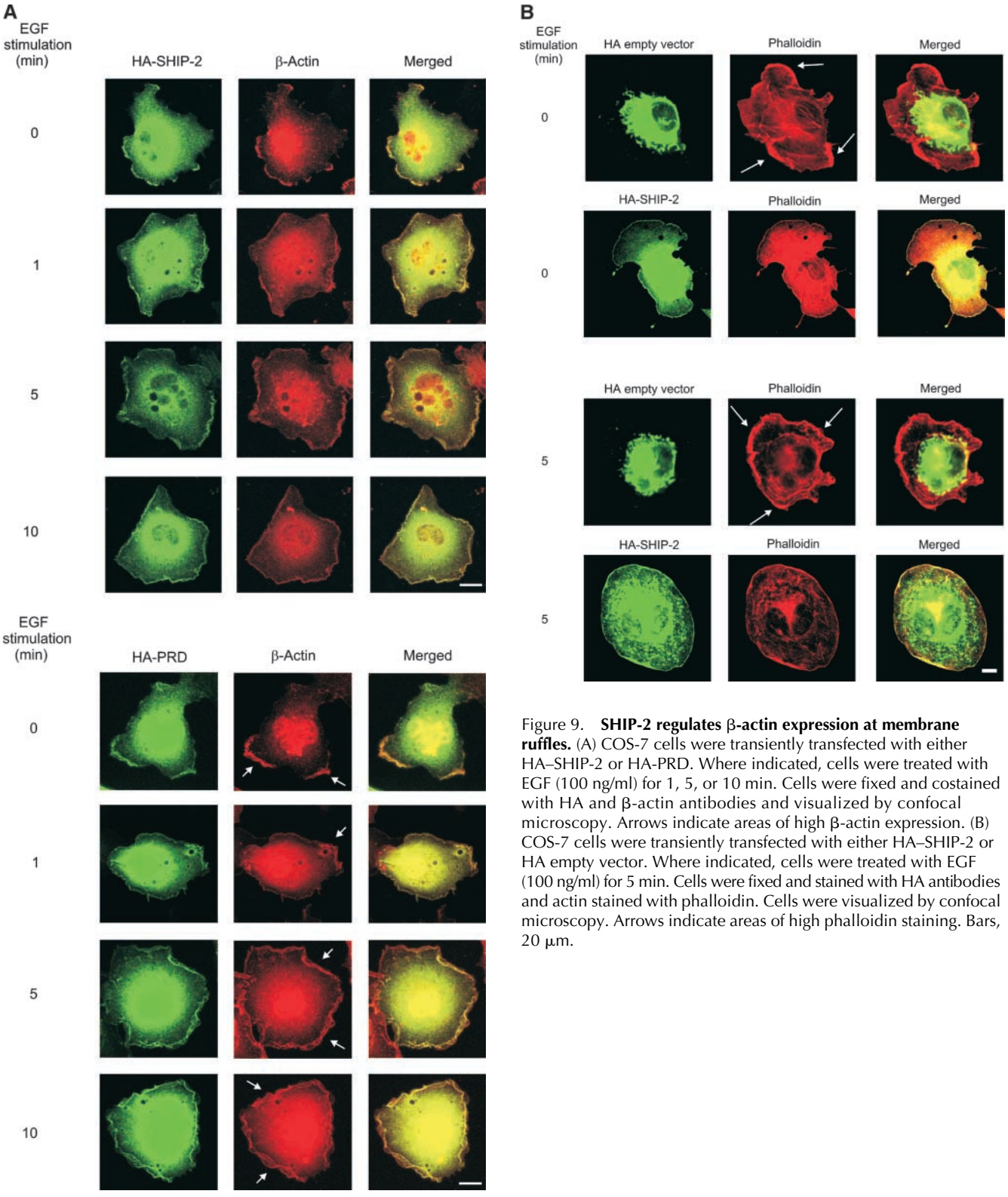

Figure 9. **SHIP-2 regulates β-actin expression at membrane ruffles.** (A) COS-7 cells were transiently transfected with either HA–SHIP-2 or HA-PRD. Where indicated, cells were treated with EGF (100 ng/ml) for 1, 5, or 10 min. Cells were fixed and costained with HA and β-actin antibodies and visualized by confocal microscopy. Arrows indicate areas of high β-actin expression. (B) COS-7 cells were transiently transfected with either HA–SHIP-2 or HA empty vector. Where indicated, cells were treated with EGF (100 ng/ml) for 5 min. Cells were fixed and stained with HA antibodies and actin stained with phalloidin. Cells were visualized by confocal microscopy. Arrows indicate areas of high phalloidin staining. Bars, 20 μm.

Role of SHIP-2 association with FLNC in insulin signaling

The recent characterization of SHIP-2 homozygous null mice has demonstrated that this 5-phosphatase plays a significant role in regulating insulin sensitivity (Clement et al., 2001). Although the signaling pathways mediating the phenotype of insulin hypersensitivity have yet to be fully determined, insulin-stimulated GLUT4 translocation to the plasma membrane appears to be enhanced in mice lacking SHIP-2. In addition, overexpression of SHIP-2, but not catalytically inactive SHIP-2, in 3T3-L1 adipocytes results in negative regulation of insulin-induced signaling (Wada et al., 2001). The submembraneous actin microfilament network links various signaling proteins, including IRS-1 and PI-3 kinase, that regulate GLUT4 translocation to the plasma membrane. Insulin-induced reorganization of the subplasma membrane actin filaments may allow exocytic GLUT4 vesicles to fuse with the plasma mem-

brane during stimulation by insulin (Khayat et al., 2000). GLUT4 expression is restricted to muscle and adipose tissue. Insulin-stimulated glucose disposal in skeletal muscle accounts for 80% of glucose uptake postprandial (Khayat et al., 2000), localizing GLUT4 to the sarcolemma. Filamin may provide a scaffold for the juxtaposition of SHIP-2 to the sarcolemma, localizing the enzyme to PtdIns(3,4,5)P_3 after insulin treatment and thereby regulating GLUT4 translocation.

Filamin forms a scaffold for the binding of Rho GTPases, including Rac1, Cdc42, Rho A, and RalA, and their activators such as Trio, a Rho guanine nucleotide exchange factor (GEF) (Ohta et al., 1999). The localization of both Rho GTPases and their activators on filamin may allow spatial coordination of actin nucleation at sites where newly assembled actin filaments are cross-linked. It is noteworthy that many filamin-binding proteins, including Trio and SHIP-2, bind to the extreme COOH-terminal repeats 21–24 of filamin, by a variety of interacting modules, including proline-rich domains, as is the case for SHIP-2 and PH domains as shown for Trio. This would therefore provide close proximity between all these signaling proteins, including SHIP-2, that regulate actin polymerization on a filamin scaffold.

Several recent studies in fibroblasts and the neutrophil cell line HL60 have demonstrated using the PH domain of PtdIns(3,4,5)P_3-binding proteins fused to GFP, that PI-3 kinase signals are generated at the leading edge of the cell (Blomberg et al., 1999; Watton and Downward, 1999; Balla et al., 2000; Servant et al., 2000). These PH domains function as an accurate probe for the localized agonist-dependent accumulation of PtdIns(3,4,5)P_3. It has been proposed, but not previously shown, that this asymmetric distribution of PtdIns(3,4,5)P_3 may result from its localized synthesis or degradation (Rickert et al., 2000). The results of the study reported here are consistent with this contention. We have shown the spatially controlled synthesis of PtdIns(3,4,5)P_3 at membrane ruffles is regulated by the PtdIns(3,4,5)P_3 5-phosphatase SHIP-2, which also localizes to membrane ruffles.

We have demonstrated SHIP-2 localization to membrane ruffles is mediated by its COOH-terminal proline-rich domain binding to the actin binding protein filamin. The expression of SHIP-2 in filamin deficient cells is exclusively cytosolic. In addition, SHIP-2 membrane localization appears to contribute to localized PtdIns(3,4,5)P_3 hydrolysis. SHIP-2 COOH-terminal truncation mutants were not as efficient at regulating PtdIns(3,4,5)P_3 at membrane ruffles as intact SHIP-2. Furthermore, displacement of endogenous SHIP-2 by overexpression of the SHIP-2 filamin binding domain (myc filamin aa 2434–2705) lead to the marked enhancement of the PI-3 kinase signal PtdIns(3,4,5)P_3. Several recent reports have shown the membrane localization of the highly related SHIP-2 homologue SHIP-1 is also important for PtdIns(3,4,5)P_3 hydrolysis (Phee et al., 2000). Enforced plasma membrane localization of SHIP-1, mediated by overexpression of a human CD8–SHIP-1 chimera, decreased the total cellular levels of PtdIns(3,4,5)P_3. Membrane targeting of SHIP-1 mediated by the COOH-terminal proline-rich domain appears to be important in B cell inhibitory function (Aman et al., 2000). In addition, the SHIP-1 COOH terminus is essential for PtdIns(3,4,5)P_3 hydrolysis and inhibition of mast cell degranulation (Damen et al., 2001). Collectively, these studies show membrane targeting of these two 5-phosphatases mediated by their respective COOH-terminal proline-rich domains plays an important functional role in regulating PI-3 kinase signals.

SHIP-2 associates with the $p130^{Cas}$ adaptor protein at focal adhesions and regulates cell spreading, which is dependent on the SHIP-2 SH2 domain and is enhanced by tyrosine phosphorylation and cell adhesion (Prasad et al., 2001). We have shown SHIP-2 and filamin also form a functionally significant complex both in the resting cells and after cellular activation at membrane ruffles. We therefore propose the binding of SHIP-2 to filamin provides a mechanism for exquisite localized hydrolysis of PtdIns(3,4,5)P_3 in resting, growth factor– and insulin–stimulated cells at the leading edge of cell.

Materials and methods

Restriction and DNA-modifying enzymes were obtained from New England Biolabs, Inc., Fermentas, or Promega. Big dye terminator cycle sequencing was from PE Applied Systems. Synthetic peptides were from Chiron Mimotopes. COS-7 cells were purchased from the American Type Culture Collection. M2 and A7 cell lines were a gift from Dr. T. Stossel (Brigham and Women's Hospital, Boston, MA). Oligonucleotides were obtained from Bresatec and the Department of Microbiology, Monash University, Melbourne, Australia. Partially purified rabbit polyclonal antibodies to human filamin B were a gift from Dr. Dominic Chung (Department of Biochemistry, University of Washington School of Medicine, WA). Goat polyclonal antibodies to chicken gizzard filamin and monoclonal antibodies to α-actinin (α-actinin) and FLAG were obtained from Sigma-Aldrich. Monoclonal antibodies to HA were obtained from Silenus, GFP antibodies were from Boehringer, β-actin antibodies were from Sigma-Aldrich, and antifilamin antibodies (raised to platelet filamin) were from Chemicon. Phalloidin stain was obtained from Molecular Probes. The GFP-PH/ARNO construct was a gift from Dr. Tamas Balla (National Institutes of Health, Bethesda, MD). The yeast two-hybrid system Matchmaker 3 and the pEGFP-C2 vector were obtained from CLONTECH Laboratories, Inc. and the pCGN vector was a gift from Dr. Tony Tiganis (Monash University, Melbourne, Australia). pEFBOS-Myc and pEFBOS-FLAG vectors were a gift from Dr. Tracey Willson (Walter and Eliza Hall Institute of Medical Research, Melbourne, Australia). Filamin A and B cDNAs were a gift from Dr. Joe Trapani and Kylie Browne (Peter MacCallum Cancer Institute, Melbourne, Australia). All other reagents were from Sigma-Aldrich unless otherwise stated.

Production of antipeptide antibodies

SHIP-2 antipeptide antibodies were generated to a fusion peptide comprising the NH_2-terminal seven amino acids of SHIP-2 fused to the COOH-terminal seven amino acids of SHIP-2 (MASACGADTLQLSK) (SHIP-2NC), or to the amino acid sequence, 1019–1030 (ITVPAPQLGHHRH) (SHIP-2P). SHIP-2NC antibodies were used for all experiments except indirect immunofluorescence of COS-7, M2, and A7 cells in which the SHIP-2P antibody was used. Peptide conjugated to diphtheria toxoid was injected subcutaneously into female New Zealand white rabbits. Affinity-purified antipeptide antibodies were obtained by chromatography of immune sera on the specific peptide coupled to thiopropyl-Sepharose 6B resin. After extensive washing, specific antibodies were eluted from the column with 0.1 M glycine-HCl, pH 2.5.

Generation of full-length SHIP-2 and SHIP-2 truncation mutants

Human SHIP-2 cDNA was generated by ligation of EST aa 279072 to the cDNA encoding INPPL-1, obtained from Dr. James Hejna (Oregon Health Sciences University, Portland, OR) (Hejna et al., 1995). Several rounds of PCR amplification enabled prolongation of the 5′-end of the clone to encompass SHIP-2 nucleotides 257–3988, which correspond to aa 16–1258 plus a COOH-terminal hexa-His-tag. SHIP-2 cDNA was cloned in-frame into pCGN (XbaI site), pEGFP-C2 (EcoRI site) and pEFBOS (MluI site) vectors, that encode for HA, GFP, and FLAG-tagged SHIP-2 fusion proteins, respectively, using PCR amplification with the introduction of specific restriction sites. Truncation mutants of SHIP-2 were also generated and were subsequently cloned into the XbaI site of pCGN. The oligonucleotide sequences and a description of the constructs generated are listed in Table I. Fidelity of all PCR products and the final constructs was confirmed by dideoxy sequencing.

Table II. **Oligonucleotides used for the generation of FLNC truncation mutants in pGADT7**

Name of construct	5′ oligonucleotide	3′ oligonucleotide	FLNC polypeptide expressed
pFLNCΔR24	5′-cgaattctgctacgtctctgagctg-3′	5′-cgaattctcaggcatctgaggagaactt-3′	Nucleotides 2,434–2,476 of repeat 22 and 23 and Hinge II region; aa 2,654–2,705
pFLNCΔH2ΔR24	5′-cgaattctgctacgtctctgagctg-3′	5′-cgaattctcacagcctcggaccagtgac-3′	Nucleotides 2,434–2,476 of repeat 22 and 23; aa 2,434–2,578
pFLNCΔR22	5′-cgaattcatgcccttcaagatccgcgttg-3′	5′-ggaattctcaagggaccttgactttg-3′	Repeat 23 and 24 and Hinge II region; aa 2,471–2,705
pFLNCR23H2	5′-cgaattcatgcccttcaagatccgcgttg-3′	5′-cgaattctcaggcatctgaggagaactt-3′′	Repeat 23 and Hinge II region; aa 2,471–2614
pFLNCR22 alone	5′-cgaattctgctacgtctctgagctg-3′	5′-gaattctcaagcctggctctgctcccc-3′	Nucleotides 2,434–2,476 of repeat 22; aa 2,434–2,481
pFLNCR23 alone	5′-cgaattcatgcccttcaagatccgcgttg-3′	5′-cgaattctcacagcctcggaccagtgac-3′	Repeat 23; aa 2,471– to 2,577
pFLNC24 alone	5′-cgaattcatgagctacagctccatcccc-3′	5′-cgaattctcaagggaccttgactttg-3′	Repeat 24; aa 2,602–to 2,705

Yeast two-hybrid analysis

The yeast two-hybrid Matchmaker III GAL4-based system was used for all yeast two-hybrid studies. The proline-rich domain of human SHIP-2 comprising nucleotides 3017–3989 (aa 936–1258), was cloned into the EcoRI site of pGBKT7, creating a GAL4 fusion protein, the "bait." "Bait" protein-expressing yeast (AH109) were transformed with human skeletal muscle cDNA library (CLONTECH Laboratories, Inc.) according to the manufacturer's guidelines. Yeast plasmid was extracted from positive clones as described (Ausubel et al., 1991).

SHIP-2 proline-rich domain–expressing yeast were transformed with filamin A and B isoforms cDNA (aa 2171–2647 and 2130–2602, respectively) to investigate an interaction. Specificity of the interactions with the SHIP-2 proline-rich domain was confirmed using a p53 "bait." In addition, a "bait" lacking the proline-rich domain of SHIP-2, but containing the SH2 domain and 5-phosphatase domain (comprising nucleotides 210–3016) was constructed using a PCR based strategy and was also used as a negative control "bait."

Immunoblot of endogenous SHIP-2, HA, and GFP-tagged SHIP-2 constructs

M2 and A7 cells were maintained as described (Cunningham et al., 1992; Ohta et al., 1999). COS-7 cells were maintained in DME, 10% (vol/vol) fetal calf serum containing 2 mM glutamine, and transfected using the DEAE-dextran procedure and allowed to grow for 2 d (Sambrook and Russel, 2001). Cells were washed briefly with PBS and treated with lysis buffer (50 mM Tris, pH 8.0, 150 mM NaCl, 1% Triton X-100, 2 mM EDTA (ethylenediaminetetraacetic acid DI-sodium salt), 1 mM benzamidine, 2 mM phenylmethylsulfonylfluoride, 2 μg/ml leupeptin, and 2 μg/ml aprotinin) for 2 h at 4°C. Lysates were centrifuged at 15,400 *g* for 10 min to obtain the Triton X-100–soluble supernatant which was analyzed by immunoblot analysis using antibodies to the specific tag, affinity-purified SHIP-NC sera, or antifilamin antibodies.

Intracellular localization of SHIP-2 in COS-7 cells

COS-7 cells were transiently transfected with GFP–SHIP-2, Myc-filamin, HA–SHIP-2, HA-SHIP-2ΔPRD, HA–SHIP-2ΔSH2, or HA-PRD truncation mutants (Table I), fixed/permeabilized, and stained. Alternatively, in some studies, 24 h after transfection, cells were placed in DME containing 0.1% FCS and 2 mM glutamate for a period of ~15 h and then stimulated with EGF (100 ng/ml). Cells expressing GFP-tagged proteins were gently washed with PBS and fixed with 3.7% formaldehyde. Cells expressing Myc and HA-tagged proteins were gently washed with PBS and then fixed and permeabilized for 10 min in PBS with 3.7% formaldehyde and 0.2% Triton X-100. Expression of Myc and HA-tagged proteins was localized using Myc and HA monoclonal antibodies and detected using tetramethylrhodamine isothiocyanate–conjugated TRITC anti–mouse IgG and fluorescein isothiocyanate–conjugated FITC anti–mouse IgG, respectively. Endogenous SHIP-2 was detected in nontransfected and Myc-filamin–transfected cells using the SHIP-2P antibody and FITC anti–rabbit IgG. Colocalization was performed using antibodies to filamin B detected with tetramethylrhodamine isothiocyanate–conjugated TRITC anti–rabbit IgG and specific actin markers, either phalloidin staining and/or antibodies to β-actin detected using TRITC anti–mouse IgG. Coverslips were mounted using SlowFade and visualized by confocal microscopy.

Immunoprecipitations

COS-7 cells were transfected via electroporation (Sambrook and Russel, 2001) and either harvested in lysis buffer 48 h posttransfection or EGF stimulated for 1 or 5 min as outlined above and harvested. Transfected and nontransfected cells were harvested and Triton X-100 extracted as outlined above. Triton X-100–soluble lysates were immunoprecipitated with either 10 μg of monoclonal FLAG or HA antibody, 5 μg of polyclonal anti–SHIP-2NC sera or preimmune sera and 60 μl of 50% slurry of protein A–Sepharose. Immunoprecipitates were immunoblotted with either FLAG, Myc, or filamin monoclonal antibodies.

Intracellular localization of SHIP-2 in A7 and M2 cells

Human filamin–deficient melanoma cell line (M2) and full-length filamin replete cell line (A7) were maintained as described (Cunningham et al., 1992; Ohta et al., 1999). Endogenous SHIP-2 was localized in resting and EGF-treated A7 and M2 cells as described above for COS-7 cells.

Assessment of β-actin, phalloidin, or GFP-PH/ARNO staining

COS-7 cells were transiently transfected via DEAE dextran-chloroquine with HA–SHIP-2 or HA-PRD, stimulated for 5 min with EGF (100 ng/ml), and costained with HA- and β-actin–specific antibodies, as outlined above. Cells were assessed for β-actin staining at the plasma membrane as a percentage of the total transfected cells. COS-7 cells were transiently transfected with HA–SHIP-2 or empty vector HA, stimulated for 5 min with EGF (100 ng/ml), and costained with HA antibodies and phalloidin. Cells were scored for phalloidin staining. COS-7 cells were transiently cotransfected with HA–SHIP-2, HA-SHIP2ΔPRD, or HA-PRD, or myc-filamin and GFP fused to the PH domain of ARNO, (GFP-PH/ARNO), or empty vector HA and GFP-PH/ARNO, stimulated for 5 min with EGF (100 ng/ml), and stained with HA antibody as outlined above. Cells were assessed for GFP-PH/ARNO expression at the plasma membrane. Approximately 40 cells were scored by an independent observer for each experiment.

Generation of FLNC truncation mutants

A PCR-based strategy was employed to generate FLNC truncation mutants which were subcloned into the EcoRI site of pGADT7, creating HA-tagged GAL4 recombinant proteins. The oligonucleotide and construct descriptions are given in Table II. Nucleotides 2,434–3,252 of FLNC was subcloned into the XbaI site and MluI site of pCGN and pEFBOS-Myc tagged, respectively. Fidelity of all PCR products and the final constructs were confirmed by dideoxy sequencing.

Localization of SHIP-2 and filamin in murine heart and soleus muscle

Mice were killed humanely following National Health and Medical Research Council guidelines, Monash University animal ethics number BAM/B/2000/17. Murine heart and soleus were dissected from 12-wk-old male mice, C57B/6. Organs were snap frozen in isopentane chilled with liquid nitrogen and blocked in OCT (10.24% wt/wt polyvinyl alcohol, 4.26% wt/wt polyethylene glycol, and 85.5% wt/wt nonreactive ingredients) compound and stored at −70°C until used. Blocks were equilibrated to −20°C before sectioning. Cross-sections and longitudinal sections were cut 7-μm thick and placed on superfrost plus slides before staining. They were then fixed in PBS/4% paraformaldehyde for 5 min at room temperature, washed with PBS, then blocked and permeablized with PBS, 10% horse serum, and 0.1% Triton X-100 for 15 min at room temperature. Slides were washed and stained with anti–SHIP-2NC sera, and detected with FITC anti–rabbit IgG. Antifilamin was detected with TRITC anti–goat IgG and anti–α-actinin was detected with TRITC anti–rabbit IgG; overnight incubation at 4°C. Sections were washed with PBS, mounted using SlowFade, and visualized by confocal microscopy.

We thank Drs. Tony Tiganis, Raju Gurung, and Susan Brown (Monash University, Clayton, Australia) for advice and helpful discussions; and Meagan McGrath and all members of the Mitchell laboratory for technical advice. Confocal images were obtained at the Biomedical Confocal Imaging Facility of Monash University.

Cindy O'Malley was funded by an Anti-Cancer Council of Victoria scholarship. This work was funded by the National Health and Medical Research Council of Australia.

Submitted: 2 April 2001
Revised: 28 September 2001
Accepted: 19 October 2001

References

Aman, M.J., S.F. Walk, M.E. March, H.P. Su, D.J. Carver, and K.S. Ravichandran. 2000. Essential role for the C-terminal noncatalytic region of SHIP in FcγRIIB1-mediated inhibitory signaling. *Mol. Cell. Biol.* 20:3576–3589.

Ausubel, F.M., R. Brent, R.E. Kingston, D.D. Moore, J.G. Seidman, J.A. Smith, and K. Struhl. 1991. Current protocols in molecular biology. John Wiley and Sons, Inc., New York.

Balla, T., T. Bondeva, and P. Varnai. 2000. How accurately can we image inositol lipids in living cells? *Trends Pharmacol. Sci.* 21:238–241.

Blero, D., F. De Smedt, X. Pesesse, N. Paternotte, C. Moreau, B. Payrastre, and C. Erneux. 2001. The SH2 domain containing inositol 5-phosphatase SHIP2 controls phosphatidylinositol 3,4,5-trisphosphate levels in CHO-IR cells stimulated by insulin. *Biochem. Biophys. Res. Commun.* 282:839–843.

Blomberg, N., E. Baraldi, M. Nilges, and M. Saraste. 1999. The PH superfold: a structural scaffold for multiple functions. *Trends Biochem Sci.* 24:441–445.

Cantley, L.C., and B.G. Neel. 1999. New insights into tumor suppression: PTEN suppresses tumor formation by restraining the phosphoinositide 3-kinase/AKT pathway. *Proc. Natl. Acad. Sci. USA.* 96:4240–4245.

Clement, S., U. Krause, F. Desmedt, J.-F. Tanti, J. Behrends, X. Pesesse, T. Sasaki, J. Penninger, M. Doherty, W. Malaisse, et al. 2001. The lipid phosphatase SHIP2 controls insulin sensitivity. *Nature.* 409:92–97.

Corvera, S., A. D'Arrigo, and H. Stenmark. 1999. Phosphoinositides in membrane traffic. *Curr. Opin. Cell Biol.* 11:460–465.

Cunningham, C.C., J.B. Gorlin, D.J. Kwiatkowski, J.H. Hartwig, P.A. Janmey, H.R. Byers, and T.P. Stossel. 1992. Actin-binding protein requirement for cortical stability and efficient locomotion. *Science.* 255:325–327.

Damen, J.E., M.D. Ware, J. Kalesnikoff, M.R. Hughes, and G. Krystal. 2001. SHIP's C-terminus is essential for its hydrolysis of PIP3 and inhibition of mast cell degranulation. *Blood.* 97:1343–1351.

Datta, S.R., A. Brunet, and M.E. Greenberg. 1999. Cellular survival: a play in three Akts. *Genes Dev.* 13:2905–2927.

Fedorov, A.A., E. Fedorov, F. Gertler, and S.C. Almo. 1999. Structure of EVH1, a novel proline-rich ligand-binding module involved in cytoskeletal dynamics and neural function. *Nat. Struct. Biol.* 6:661–665.

Gorlin, J.B., R. Yamin, S. Egan, M. Stewart, T.P. Stossel, D.J. Kwiatkowski, and J.H. Hartwig. 1990. Human endothelial actin-binding protein (ABP-280, nonmuscle filamin): a molecular leaf spring. *J. Cell Biol.* 111:1089–1105.

Habib, T., J.A. Hejna, R.E. Moses, and S.J. Decker. 1998. Growth factors and insulin stimulate tyrosine phosphorylation of the 51C/SHIP2 protein. *J. Biol Chem.* 273:18605–18609.

Hejna, J.A., H. Saito, L.S. Merkens, T.V. Tittle, P.M. Jakobs, M.A. Whitney, M. Grompe, A.S. Friedberg, and R.E. Moses. 1995. Cloning and characterization of a human cDNA (INPPL1) sharing homology with inositol polyphosphate phosphatases. *Genomics.* 29:285–287.

Hughes, W.E., F.T. Cooke, and P.J. Parker. 2000. Sac phosphatase domain proteins. *Biochem. J.* 350:337–352.

Ijuin, T., Y. Mochizuki, K. Fukami, M. Funaki, T. Asano, and T. Takenawa. 2000. Identification and characterization of a novel inositol polyphosphate 5-phosphatase. *J. Biol. Chem.* 275:10870–10875.

Ishihara, H., T. Sasaoka, H. Hori, T. Wada, H. Hirai, T. Haruta, W.J. Langlois, and M. Kobayashi. 1999. Molecular cloning of rat SH2-containing inositol phosphatase 2 (SHIP2) and its role in the regulation of insulin signaling. *Biochem. Biophys. Res. Commun.* 260:265–272.

Khan, A.H., D.C. Thurmond, C. Yang, B.P. Ceresa, and J.E. Pessin. 2000. Munc18c regulates insulin-stimulated GLUT4 translocation to the transverse tubules in skeletal muscle. *J. Biol. Chem.* 38:12.

Khayat, Z.A., P. Tong, K. Yaworsky, R.J. Bloch, and A. Klip. 2000. Insulin-induced actin filament remodeling colocalizes actin with phosphatidylinositol 3-kinase and GLUT4 in L6 myotubes. *J. Cell Sci.* 113:279–290.

Kisseleva, M.V., M.P. Wilson, and P.W. Majerus. 2000. The isolation and characterization of a cDNA encoding phospholipid-specific inositol polyphosphate 5-phosphatase. *J. Biol. Chem.* 275:20110–20116.

Maestrini, E., C. Patrosso, M. Mancini, S. Rivella, M. Rocchi, M. Repetto, A. Villa, A. Frattini, M. Zoppe, P. Vezzoni, et al. 1993. Mapping of two genes encoding isoforms of the actin binding protein ABP-280, a dystrophin like protein, to Xq28 and to chromosome 7. *Hum. Mol. Genet.* 2:761–766.

Majerus, P.W. 1996. Inositols do it all. *Genes Dev.* 10:1051–1053.

Malecz, N., P.C. McCabe, C. Spaargaren, R. Qiu, Y. Chuang, and M. Symons. 2000. Synaptojanin 2, a novel rac1 effector that regulates clathrin-mediated endocytosis. *Curr. Biol.* 10:1383–1386.

Martin, T.F. 1997. Phosphoinositides as spatial regulators of membrane traffic. *Curr. Opin. Neurobiol.* 7:331–338.

Mochizuki, Y., and T. Takenawa. 1999. Novel inositol polyphosphate 5-phosphatase localizes at membrane ruffles. *J. Biol. Chem.* 274:36790–36795.

Ohta, Y., N. Suzuki, S. Nakamura, J.H. Hartwig, and T.P. Stossel. 1999. The small GTPase RalA targets filamin to induce filopodia. *Proc. Natl. Acad. Sci. USA.* 96:2122–2128.

Ooms, L.M., B.K. McColl, F. Wiradjaja, A.P. Wijayaratnam, P. Gleeson, M.J. Gething, J. Sambrook, and C.A. Mitchell. 2000. The yeast inositol polyphosphate 5-phosphatases np52p and np53p translocate to actin patches following hyperosmotic stress: mechanism for regulating phosphatidylinositol 4,5-bisphosphate at plasma membrane invaginations. *Mol. Cell. Biol.* 20:9376–9390.

Pesesse, X., S. Deleu, F. De Smedt, L. Drayer, and C. Erneux. 1997. Identification of a second SH2-domain-containing protein closely related to the phosphatidylinositol polyphosphate 5-phosphatase SHIP. *Biochem. Biophys. Res. Commun.* 239:697–700.

Pesesse, X., V. Dewaste, F. De Smedt, M. Laffargue, S. Giuriato, C. Moreau, B. Payrastre, and C. Erneux. 2001. The SH2 domain containing inositol 5-phosphatase SHIP2 is recruited to the EGF receptor and dephosphorylates phosphatidylinositol 3,4,5-trisphosphate in EGF stimulated COS-7 cells. *J. Biol. Chem.* 10:10.

Phee, H., A. Jacob, and K.M. Coggeshall. 2000. Enzymatic activity of the Src homology 2 domain-containing inositol phosphatase is regulated by a plasma membrane location. *J. Biol. Chem.* 275:19090–19097.

Prasad, N., R.S. Topping, and S.J. Decker. 2001. SH2-containing inositol 5′-phosphatase SHIP2 associates with the p130(Cas) adapter protein and regulates cellular adhesion and spreading. *Mol. Cell. Biol.* 21:1416–1428.

Rickert, P., O.D. Weiner, F. Wang, H.R. Bourne, and G. Servant. 2000. Leukocytes navigate by compass: roles of PI3Kgamma and its lipid products. *Trends Cell Biol.* 10:466–473.

Sakisaka, T., T. Itoh, K. Miura, and T. Takenawa. 1997. Phosphatidylinositol 4,5-bisphosphate phosphatase regulates the rearrangement of actin filaments. *Mol. Cell. Biol.* 17:3841–3849.

Sambrook, J., and D.W. Russel. 2001. Molecular Cloning: A Laboratory Manual. Cold Spring Harbor Laboratory Press, Cold Spring Harbor, NY.

Servant, G., O.D. Weiner, P. Herzmark, T. Balla, J.W. Sedat, and H.R. Bourne. 2000. Polarization of chemoattractant receptor signaling during neutrophil chemotaxis. *Science.* 287:1037–1040.

Stossel, T.P., J. Condeelis, L. Cooley, J.H. Hartwig, A. Noegel, M. Schleicher, S. Shapiro. 2001. Filamin as integrators of cell mechanics and signalling. *Nat. Rev.* 2:138–145.

Takafuta, T., G. Wu, G.F. Murphy, and S.S. Shapiro. 1998. Human beta-filamin is a new protein that interacts with the cytoplasmic tail of glycoprotein Ibalpha. *J. Biol. Chem.* 273:17531–17538.

Taylor, V., M. Wong, C. Brandts, L. Reilly, N.M. Dean, L.M. Cowsert, S. Moodie, and D. Stokoe. 2000. 5′ phospholipid phosphatase SHIP-2 causes protein kinase B inactivation and cell cycle arrest in glioblastoma cells. *Mol. Cell. Biol.* 20:6860–6871.

Tsujishita, Y., S. Guo, L.E. Stolz, J.D. York, and J.H. Hurley. 2001. Specificity determinants in phosphoinositide dephosphorylation: crystal structure of an archetypal inositol polyphosphate 5-phosphatase. *Cell.* 105:379–389.

van der Ven, P.F., W.M. Obermann, B. Lemke, M. Gautel, K. Weber, and D.O. Furst. 2000. Characterization of muscle filamin isoforms suggests a possible role of gamma-filamin/ABP-L in sarcomeric Z-disc formation. *Cell Motil. Cytoskeleton.* 45:149–162.

Wada, T., T. Sasaoka, M. Funaki, H. Hori, S. Murakami, M. Ishiki, T. Haruta, T. Asano, W. Ogawa, H. Ishihara, and M. Kobayashi. 2001. Overexpression of SH2-containing inositol phosphatase 2 results in negative regulation of insulin-induced metabolic actions in 3T3-L1 adipocytes via its 5′-phosphatase catalytic activity. *Mol. Cell. Biol.* 21:1633–1646.

Watton, S.J., and J. Downward. 1999. Akt/PKB localisation and 3′ phosphoinositide generation at sites of epithelial cell-matrix and cell-cell interaction. *Curr. Biol.* 9:433–436.

Whisstock, J.C., S. Romero, R. Gurung, H. Nandurkar, L.M. Ooms, S.P. Bottomley, and C.A. Mitchell. 2000. The inositol polyphosphate 5-phosphatases and the Apurinic/Apyrimidinic base excision repair endonucleases share a common mechanism for catalysis. *J. Biol. Chem.* 275:37055–37061.

Wisniewski, D., A. Strife, S. Swendeman, H. Erdjument-Bromage, S. Geromanos, W.M. Kavanaugh, P. Tempst, and B. Clarkson. 1999. A novel SH2-containing phosphatidylinositol 3,4,5-trisphosphate 5-phosphatase (SHIP2) is constitutively tyrosine phosphorylated and associated with src homologous and collagen gene (SHC) in chronic myelogenous leukemia progenitor cells. *Blood.* 93:2707–2720.

Xie, Z., W. Xu, E.W. Davie, and D.W. Chung. 1998. Molecular cloning of human ABPL, an actin-binding protein homologue. *Biochem Biophys. Res. Commun.* 251:914–919.

Xu, W., Z. Xie, D.W. Chung, and E.W. Davie. 1998. A novel human actin-binding protein homologue that binds to platelet glycoprotein Ibalpha. *Blood.* 92:1268–1276.